Nanotechnology and Precision Engineering 2 (2019) 1–7

Contents lists available at ScienceDirect

Nanotechnology and Precision Engineering

journal homepage: http://www.keaipublishing.com/en/journals/nanotechnology-and-precision-engineering/

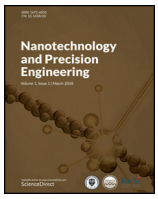

Investigation of the performance of a pilot-scale barrel atmospheric plasma system for plasma activation of polymer particles

Hisham M. Abourayana [a], Peter J. Dobbyn [a], Pat Whyte [b], Denis P. Dowling [a,*]

[a] Surface Engineering Group, School of Mechanical and Materials Engineering, University College Dublin, Belfield, Dublin 4, Ireland
[b] Irish Micro Mouldings, Inverin, Co. Galway, Ireland

ARTICLE INFO

Keywords:
Atmospheric pressure plasma
Barrel plasma reactor
Polymer particles
Water contact angle
X-ray photoelectron spectroscopy
Injection moulding

ABSTRACT

This study reports the development and performance of a pilot-scale barrel atmospheric plasma reactor for the atmospheric plasma activation treatment of polymer particles. The polymer particles treated included acrylonitrile butadiene styrene (ABS) and polypropylene (PP). These particles had diameters in the range of 3–5 mm. The initial studies were carried out using a laboratory-scale barrel reactor designed to treat polymer particle batch sizes of 20 g. A pilot-scale reactor that could treat 500 g particle batch sizes was then developed to facilitate pre-industrial-scale treatments. The effect of operating pulse density modulation (PDM) in the range 10%–100% and plasma treatment time on the level of activation of the treated polymers were then investigated. ABS revealed a larger decrease in water contact angle compared with PP after plasma treatment under the same conditions. The optimal treatment time of ABS (400 g of polymer particles) in the pilot-scale reactor was 15 min. The plasma-activated polymer particles were used to fabricate dog-bone polymer parts through injection molding. Mechanical testing of the resulting dog-bone polymer parts revealed a 10.5% increase in tensile strength compared with those fabricated using non-activated polymer particles.

1. Introduction

Polymers are often processed as particles such as for use in 3D printing, injection molding, and biotechnology.[1–3] Surface properties have been demonstrated to be of key importance to the performance of polymer particles.[4] Plasma treatments have been extensively applied to enhance the surface properties of polymer particles through the introduction of polar groups and cross-linking on the surface without affecting the bulk composition.[5,6] In contrast to flat polymeric substrates, very few publications on the atmospheric plasma treatment of polymer particles are available.[7] Amongst the plasma reactor designs for the treatment of polymer particles are fluidized bed reactors, downer reactors, and batch reactors.[8–10] However, fluidized bed systems present a number of problems when a range of particle sizes is to be treated (e.g., keeping larger particles suspended while preventing loss of smaller particles) and often require long treatment times of up to several hours.[11,12] In some reactors (i.e., downer reactors), particles pass through the plasma zone within a few milliseconds, and, thus, only a weak level of polymer activation is obtained.[13] The fluidized bed and downer reactors are difficult to apply at the industrial scale due to size limitations, as well as their high consumption of power and gas.[14] For industrial application of particle-treatment technology, a relatively large quantity of polymer particles must be treated per batch with short treatment times.

Most previous studies on the activation of polymer particles have focused on experiments using laboratory-scale particle batch sizes of a few grams.[4,14–16] This study compares the performance of a laboratory-scale atmospheric barrel plasma reactor on which we have previously reported (for treating up to 20 g of polymer particles),[17,18] with a pilot-scale barrel plasma system designed to facilitate the treatment of 500 g of polymer particles. This comparison study was carried out using acrylonitrile butadiene styrene (ABS) and polypropylene (PP) polymer particles.

2. Experimental work

Photographs of both the laboratory- and pilot-scale atmospheric barrel plasma reactors are shown in Fig. 1. The laboratory-scale reactor consists of a quartz chamber with effective treatment area dimensions of 10 cm length and 10 cm inner diameter.[17] The plasma in this reactor operates at a frequency of 20 kHz and input voltage of up to 110 V, with a maximum output power of 100 W (Plasma Technics Inc., USA). The length of the plasma chamber of the pilot-scale reactor is 35 cm, and the system is driven by a 1500 W high-voltage power source (Plasma Technics Inc., USA). In this system, by varying the percent ON time vs OFF time (pulse density modulation (PDM)%) from 1% to 100%, the output power can be controlled. In both reactors, the high-voltage power

* Corresponding author.
E-mail address: denis.dowling@ucd.ie (D.P. Dowling).

https://doi.org/10.1016/j.npe.2019.03.002

Fig. 1. Photographs of laboratory scale reactor (left) and pilot-scale reactors (right).

source is directly connected to two aluminum rods acting as the biased and earthed electrodes; these rods are also used to rotate the plasma chamber to agitate the particles during treatment. Helium was investigated as a process gas, and its flow rate was controlled using MASS-VIEW MV-394-He rotameter from Bronkhorst. The two-barrel chambers were purged for 5 min with helium with rotation of the polymer particles prior to plasma ignition. Plasma activation studies were carried out using commercial ABS and PP polymer particles manufactured by LG Chem and INEOS Olefins & Polymer Europe, respectively. The cylindrical ABS particles had a diameter of 2 mm and height of 3 mm, while the PP particles had an elliptical shape with diameters of 3 and 2 mm and a height of 1 mm.

The level of polymer particle activation after plasma treatment was evaluated based on water contact angle (WCA) measurements obtained using an OCA 20 video capture apparatus from Dataphysics Instruments. WCAs were measured both immediately and at varying times after plasma treatment to determine the rate of hydrophobic recovery. This procedure was achieved by applying water drops of 0.5 μL to the particle surfaces. X-ray photoelectron spectroscopy (XPS) analysis was carried out using an Axis Ultra spectrometer (Kratos Analytical) with a monochromated Al Kα X-ray source. This technique was used to investigate changes in surface chemistry after plasma treatment of both ABS and PP. Optical emission spectroscopy (OES) was used as a diagnostic tool to monitor changes in atomic and molecular species in response to changes in the experimental conditions. In this study, spectra from the plasma discharge were obtained in the 200–850 nm region using an Ocean Optics USB4000 UV/VIS spectrometer. A VarioCam high-resolution infrared thermographic camera used to measure the plasma chamber temperature.

A Battenfeld 250 Plus injection-molding machine was used to produce tensile test (dog-bone) specimens with standard dimensions according to ASTM D1708-13 from both non- and plasma-activated ABS polymer particles. Tensile testing of the dog-bone samples was carried out using a Hounsfield universal testing machine equipped with a 10 kN load cell. Tensile test measurements were carried out at a rate of 5 mm/min.

3. Results and discussion

This section considers the plasma and thermal measurements obtained for both laboratory- and pilot-scale barrel sources, as well as their effectiveness for the plasma activation of polymer particles.

3.1. Optical emission spectroscopy analysis and thermal measurements

OES was used to examine the emission spectra obtained from the laboratory- and pilot-scale reactors in the range of 250–850 nm (Fig. 2). The spectra contained the molecular bands of hydroxyl OH (A–X) at 307 nm; nitrogen N_2 (C– B) second positive system at 337, 358 and 380 nm; and N_2^+ (B–X) first negative system at 391 nm, as well as the excited atomic emission lines of helium He I transition $3s^3S^1 \rightarrow 2p^3P^0$ at 706 nm and oxygen O I transition $3p^5P \rightarrow 3s^5S^0$ at 777 nm.[19,20] Spectral lines of helium atoms, including the He I transition

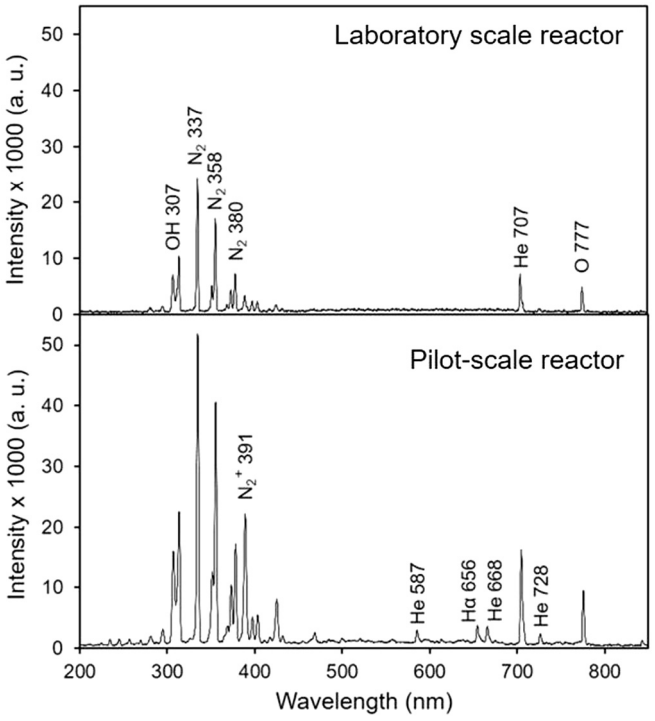

Fig. 2. Optical emission spectra obtained from laboratory scale and pilot-scale reactors. For these experiments the helium flow rate was 10 slm and the PDM% for the pilot-scale system was maintained at 40%.

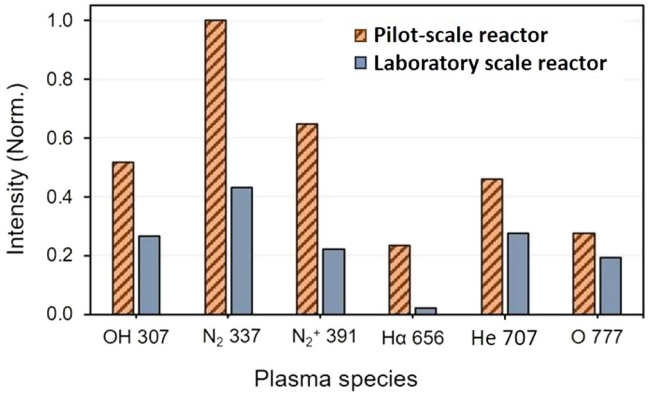

Fig. 3. Intensity ratios of the OES peak spectra obtained from both the laboratory and pilot-scale reactors. Each spectrum is normalized to the N_2 peak at 337 nm.

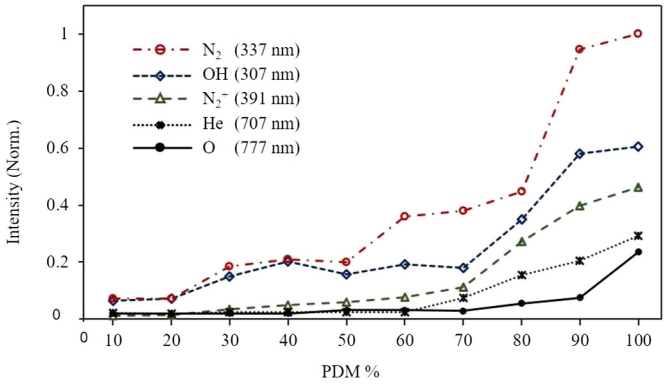

Fig. 4. Effect of PDM% on the plasma species intensities obtained by OES.

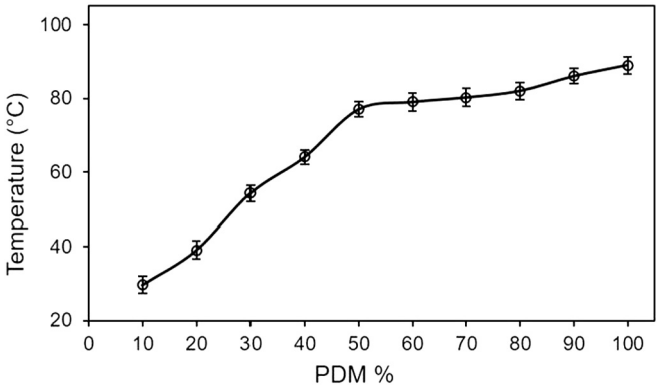

Fig. 6. Effect of plasma operating PDM on the temperature generated at the barrel glass wall surface.

$3d^3D \rightarrow 2p^3P^0$ at 587 nm, the He I transition $3d^1D \rightarrow 2p^1P^0$ at 667 nm, the He I transition $3s^1S^0 \rightarrow 2p^1P^0$ at 728 nm·Hα transition 2p-3d at 656 nm was also observed in the spectra obtained from the pilot-scale reactor. The excited species OH and N_2 are readily produced through electron-impact excitation and N_2^+ produced by the Penning ionization by helium metastables.[21] He706 is produced by radiative dissociation of the He_2 dimer, which is formed by recombination of the metastable He atom.[22] The helium emission at 706 nm indicates the presence of either highly energetic electrons or He_2^+ ions and high-energy electrons.[23,24]

To compare the intensities of the spectra formed from these two-barrel plasma reactors, integrating the area under the emission peaks was necessary. Six wavelengths were selected for this investigation, namely, 307 nm (OH), 337 nm (N_2), 391 nm (N_2^+), 656 nm (Hα), 707 nm (He), and 777 nm (O). These reactive plasma species play a significant role in determining the effectiveness of atmospheric pressure plasmas.[20,25] Normalization of the entire spectrum to the intensity of the N_2 peak at 337 nm was performed to allow examination and comparison of the intensity ratios of various peaks, thus providing better insights into the concentration of species generated within the plasma.[26] Figure 3 shows the intensity ratio of the spectra obtained from both reactors. The figure clearly demonstrates that the intensities of the spectra formed from the pilot reactor are more intense than those obtained from the laboratory-scale reactor. A probable explanation for this finding is that ionization and discharge power increase with increasing input power, leading to a corresponding increase in plasma species intensity.[19,24]

The effect of varying PDM% on the resulting plasma species intensity was investigated in the case of the pilot-scale reactor. As shown in Fig. 4, the intensity of the plasma species increased, as expected, with increasing PDM%. A probable explanation for this finding is that the applied power increases as the PDM% increases, leading to an increase in the mean energy of the electrons, which, in turn, promotes the rate of formation of plasma species.[27]

The effect of varying PDM% on the stability of the plasma generated over time in the pilot-scale reactor was also investigated. OES spectra were collected every 10 s for a total of 1 min using an integration time of 1 s. In general, the intensities of the plasma species increased with increasing PDM%. At low PDM% (i.e., <60%), the spectral intensities remained nearly unchanged over the 60 s measurement period investigated, which indicates a high degree of plasma stability. Figure 5 confirms this supposition and shows the effect of changing PDM% on the intensity of the OH (307 nm) and N_2 (337 nm) spectra in the pilot-scale reactor. The stability observed is very important for the industrial application of the developed processing treatment. The factors influencing the intensities of the excited plasma species include their energy thresholds and lifetimes.[22]

The effect of varying PDM% on the temperature generated by the pilot-scale reactor discharge on the barrel glass chamber wall was investigated using a high-resolution infrared thermographic camera (VarioCam). Thermal measurements were made every 30 s for a period of 5 min after plasma generation at different PDM%. The barrel chamber was allowed to cool to room temperature between each measurement. As shown in Fig. 6, the temperature increased with increasing PDM%, and the maximum temperature obtained at PDM% = 100% was 89 °C.

In the case of laboratory scale reactor, the temperature generated by the discharge was previously investigated using the same high-resolution infrared thermographic camera (VarioCam) 17. In this study, the temperature of the glass chamber was recorded 30 min

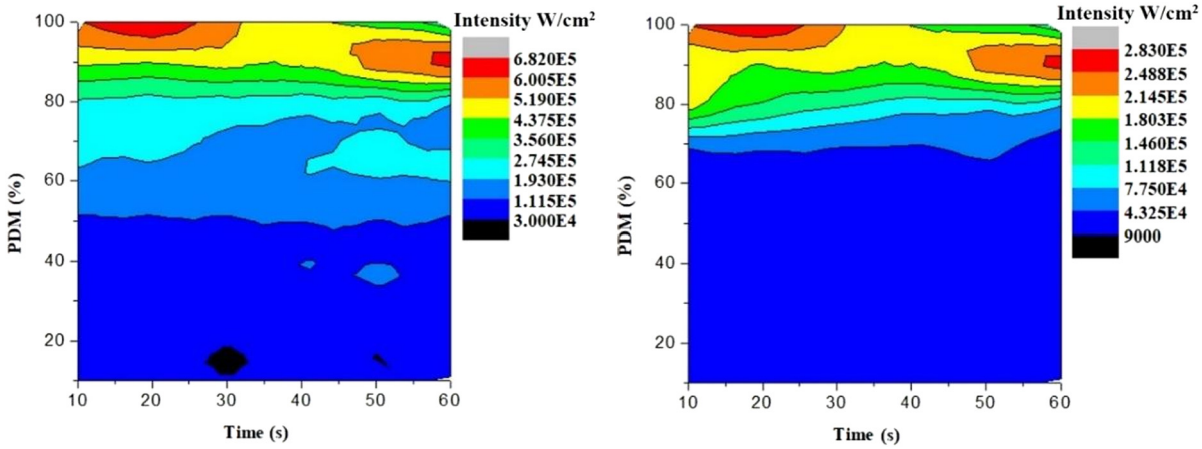

Fig. 5. Effect of PDM% on the intensity of OH spectra at 337 nm (left) and N_2 Spectra at 307 nm (right). Measurements were obtained over a 60 s period.

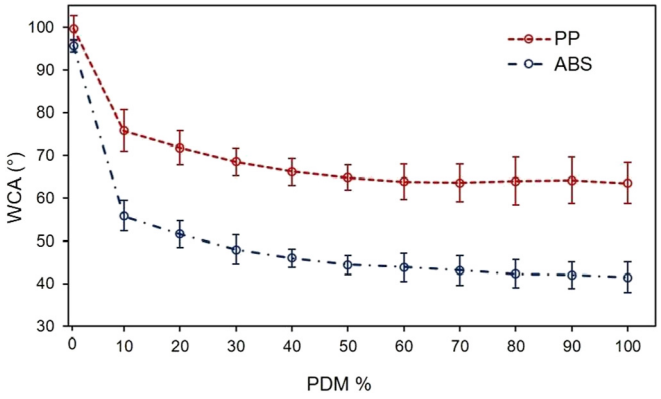

Fig. 7. Effect of plasma operating PDM on the WCAs of ABS and PP polymer particles. Note the reduction in the error bars obtained for treatments of PDM% = 40% and 50%.

after the plasma was ignited, and the maximum temperature obtained was 28.9 °C.

The higher temperature generated by the plasma inside the pilot-scale reactor compared with that in the laboratory-scale system reflects the lower discharge power generated within the latter. These temperature measurements correlate well with the data obtained via OES, and both datasets demonstrate the enhanced discharge intensity achieved using the pilot-scale reactor.

3.2. Water contact angle analysis

A screening study was carried out using the pilot-scale reactor to evaluate the effect of PDM% on the level of activation of polymer particles. The results of this study are given in Fig. 7, which demonstrates the effect of the PDM% on the WCAs of the treated ABS and PP particles.

In this study, a particle batch size of 20 g was used for all treatments. At least 35 WCA measurements were performed on randomly selected particles from each batch (one measurement per particle), and average values were calculated. Error bars were also calculated based on the standard deviation. After 30 s of plasma treatment using a helium discharge, WCAs decreased with increasing PDM%. ABS revealed a larger decrease in WCA compared with that obtained from PP after plasma treatment under the same conditions likely because of the presence of two chemical functionalities in ABS (i.e., C═C bonds and nitrile groups), as well as the lack of polar functional groups on the PP polymer chain.[28,29]

Minimum variations in WCA error bars were obtained for treatments of PDM% = 40% and 50%, which indicates that a high degree of plasma stability is obtained when the barrel reactor is operated under these processing conditions. This observation correlates well with the results of the OES measurements detailed in Fig. 5, which indicated that the spectral intensities remained nearly unchanged during the 60 s measurement period at low PDM% (<60%).

Having established that PDM% = 40% yields the lowest variation in measured WCAs, this parameter is used for helium plasma activation of ABS and PP polymer particles using the pilot-scale reactor; here, a comparison study was carried out using the results of the laboratory-scale reactor. The results of this comparison are given in Fig. 8. For the investigated treatment time of up to 5 min, a decrease in the WCAs of ABS and PP polymer particles was observed. In the case of the laboratory-scale system, the WCA decreased from 95° to 53° for ABS and from 99° to 69° for PP particles. In the case of the pilot-scale reactor, WCAs decreased to 46° and 66° for ABS and PP respectively, during the first 30 s of plasma treatment. No further significant decrease in WCA was found with longer treatment times. This finding is likely to be due to the lack of change in the oxygen content of the polymer surface as the exposure time increased.[30,31]

In the case of PP, increasing the treatment time in the pilot-scale reactor to 5 min led to a smaller increase in WCA compared with that obtained after the 2 min treatment time. This result may be due to thermal damage caused to the polymer surfaces during plasma activation. Thermal studies revealed that the maximum temperature was achieved after 5 min; here, the plasma was ignited at 64 °C under PDM% = 40%. While this temperature is significantly less than the melting temperature of PP (160 °C), the increase in WCA indicates some deterioration on the surface of the polymer.[32]

The effect of polymer quantity (by weight) treated in the barrel chambers on activation efficiency was assessed using the ABS particles. This investigation involved the treatment of polymer quantities between 20 and 500 g using both the laboratory and pilot-scale systems. As expected, activation efficiency decreased as the quantity of polymer increased due to the significantly higher surface area to be activated (Fig. 9). Over the 2 min treatment time investigated, the WCA increased from 58° to 75° in the case of the laboratory-scale reactor and from 40° to 53° in the pilot-scale reactor with increasing polymer weight.

The much smaller increase in WCA obtained with the pilot-scale reactor helps to demonstrate its enhanced plasma activation efficiency. The intense plasma obtained from the pilot-scale reactor with the generation of active species, such as OH and Hα 19, as well as its longer length (35 cm vs. 10 cm) compared with that of the laboratory-scale system play a key role in the enhanced level of polymer activation achieved.

Figure 10 shows the effect of treatment time on the WCA of 500 g batches of ABS particles in the pilot-scale reactor. WCAs decreased from 95° to 46° after 5 min of treatment and increasing the treatment time to 10 min did not yield any further significant decrease in WCA.

Plasma-activated polymer surfaces generally undergo a phenomenon called hydrophobic recovery or aging,[33] which involves an increase in the WCA of the polymer with time. This phenomenon presents an important parameter as it provides an indication of the length of time after

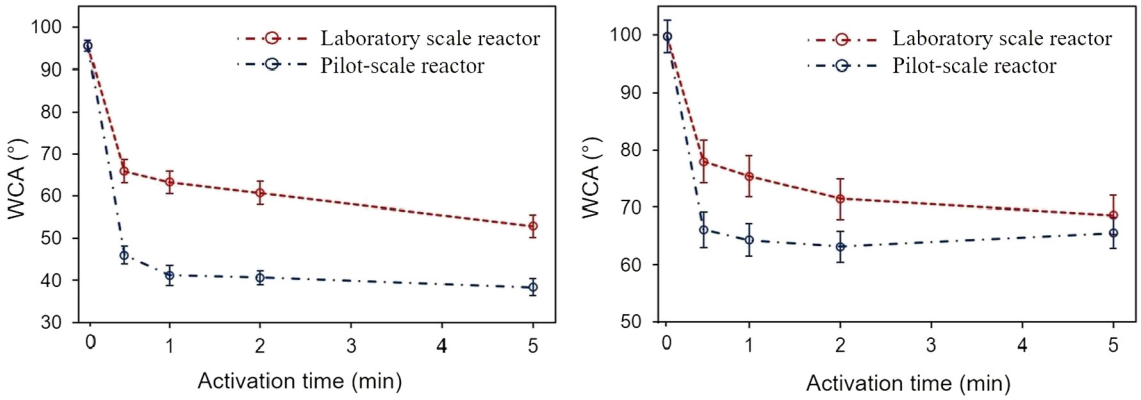

Fig. 8. Effect of plasma treatment time on WCAs of the ABS (left) and PP (right) polymer particles.

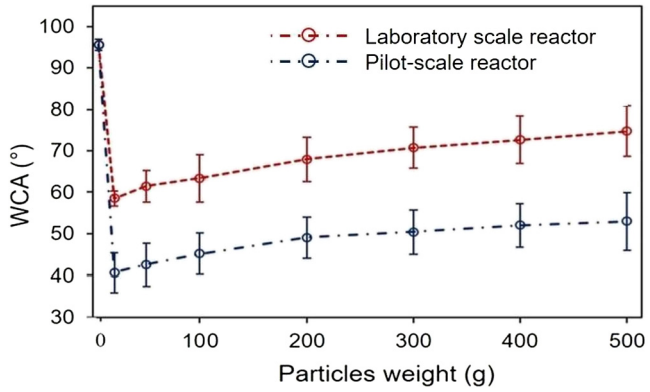

Fig. 9. Effect of increasing the weight of ABS particles on the WCA (He plasma, 2 min of treatment time).

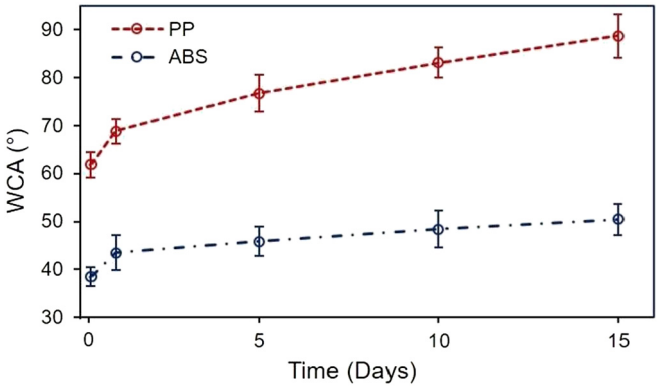

Fig. 11. Change in WCA due to hydrophobic recovery of the PP and ABS polymer particles.

treatment a polymer can remain activated. The hydrophobic recovery rates of the treated ABS and PP polymer particles were examined at intervals for up to 15 days. As shown in Fig. 11, in the case of ABS, the WCA recovered slightly from 38° to 43° after the first day of treatment and then increased to 50° after 15 days. This value is much lower than the 95° WCA obtained for the untreated polymer. By contrast, the WCA of the PP polymer particles increased to 88° after 15 days.

3.3. XPS analysis

Surface chemistry changes associated with the He plasma treatments of ABS and PP polymer particles using both the laboratory- and pilot-scale reactors were monitored using XPS. Table 1 demonstrates the elemental compositions of the ABS and PP polymer particles before and after plasma treatment using both reactors. The surfaces of both polymers are mainly composed of carbon and a small amount of oxygen. The presence of oxygen in ABS and PP may be related to additives during the manufacturing process.[29] A small amount of nitrogen was also found in ABS due to the nitrile group of acrylonitrile units. After plasma treatment, a notable reduction in carbon contents and an increase in the ratio of oxygen atoms on the ABS and PP polymer surfaces was observed. In the case of ABS, the N:C ratio also increased.

To investigate the principal functional groups introduced to the ABS and PP surfaces with helium plasma treatment, the C1s spectrum was fitted to calculate the concentration of each chemical component, as shown in Fig. 12.

The C1s core level spectrum of ABS revealed two peaks at 285 and 286.5 eV, corresponding to the C—C/C—H bonds and R—CN/C—O groups, respectively. After plasma treatment, a decrease in concentration of C—C/C—H bonds and an increase in the concentration of R—CN/C—O were observed. New functional groups related to —C═O (287.6 eV) and N—C═O (289 eV) were also found after plasma treatment. Table 2 shows the percentages of species on the ABS polymer particles before and after helium plasma treatment.

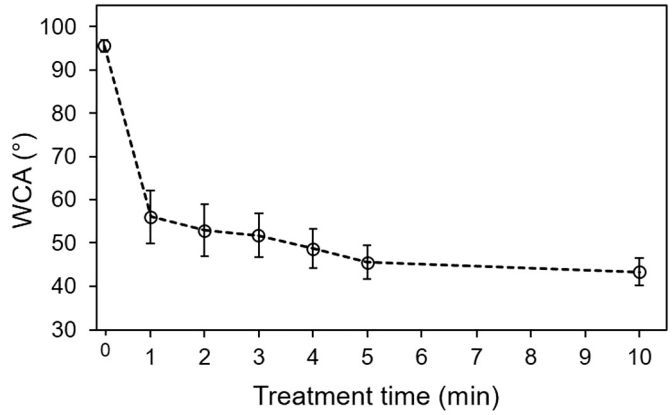

Fig. 10. Effect of plasma treatment time on WCA of 500 g batches of ABS polymer particles.

In the case of PP, the spectra of untreated particles indicate the presence of three peaks with binding energies of 285 eV for C—C/C—H, 286.6 eV for C—O, and 289 eV for O—CO—C. After plasma treatment, an increase in concentration of O—CO—O bonds was noted, and an additional peak obtained at 287.5 eV was assigned to C═O/O—C—O 28. As demonstrated in Table 3, plasma treatment of the PP surface yielded a large increase in oxygen functionality.

The results of this XPS study correlate well with the WCA data. Oxygen-containing functional groups increased the surface hydrophilicity of the polymer particles.[34] A higher concentration of oxygen species was obtained on polymer surfaces treated using the pilot-scale reactor compared with that obtained from particles treated using the laboratory-scale system.

3.4. Tensile testing

To investigate whether the atmospheric plasma treatment of polymer particles influences the mechanical performance of the resultant injection-molded ABS polymer parts, tensile testing was carried out. Plasma pre-treatment of 400 g of polymer particles was conducted using the pilot-scale reactor, and the activated particles were injection molded immediately after treatment. Measurements were obtained from batches of five injection-molded dog-bones samples, and the results were averaged to determine the maximum tensile strength in each batch. As shown in Fig. 13, the maximum increase in tensile strength of the injected molded parts was 10.5% when the treatment time was 15 min. Longer treatment time resulted in decreases in tensile strength. A possible explanation for this finding is that the polymer surfaces are modified by exposure to excessive plasma, which can leave active sites that are subject to post-reactions; this process is also called aging.[35]

A probable explanation for the increased mechanical strength of injection-molded parts after plasma treatment of the polymer particles involves the enhanced bonding achieved between the activated particles. Besides enhancing the surface energy of the polymer, plasma

Table 1
Elemental composition of ABS and PP before and after plasma treatment.

Samples		%C	%O	%N	C:O	C:N
ABS	Before treatment	92.7	2.8	3.8	33.1	24.4
	Laboratory-scale reactor	84.8	11.3	3.9	7.5	21.7
	Pilot-scale reactor	82.9	12.4	4.5	6.7	18.5
PP	Before treatment	89.7	10.1		8.8	
	Laboratory-scale reactor	87.2	12.5		6.9	
	Pilot-scale reactor	83.2	14.6		5.7	

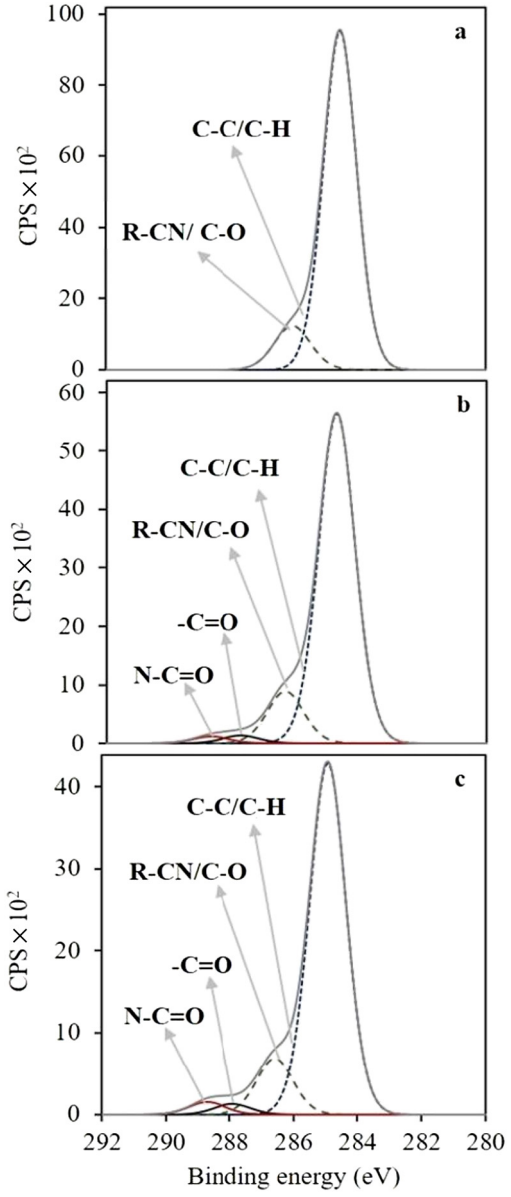

Fig. 12. C1s spectra of ABS: (a) untreated; (b) plasma treated using laboratory scale reactor and (c) plasma treated using pilot-scale reactor.

may also remove moisture or organic contaminations present on the material surface.[36,37] Similar enhancements in polymer mechanical performance have been demonstrated by our group for activated polymer particles used to produce 3D printing filaments.[38]

4. Conclusions

This study investigates the performance of laboratory and pilot-scale barrel atmospheric plasma reactors for activation of ABS and PP polymer particles; these reactors were designed to treat polymer particle batch sizes of 20 and 500 g, respectively. The influence of several parameters, including operating PDM, plasma treatment time, and increasing weight of polymer particles on the level of plasma surface activation were investigated based on WCA measurements. Comparing the laboratory- and pilot-scale reactors, the latter achieved more rapid polymer activation, as well as lower WCAs in the treated polymers. The pilot-scale reactor exhibited a much more intense helium discharge than the laboratory-scale reactor, as demonstrated by OES measurements. In the pilot-scale reactor, WCAs decreased with increasing treatment time and PDM%. XPS analysis indicated that oxygen-containing functional groups help increase the surface hydrophilicity of the polymer particles. The effect of plasma activation of the polymer particles on their mechanical performance was investigated through injection-molded plasma-activated ABS particles. The resultant dog-bone test samples were investigated using tensile strength measurements. The plasma pre-treated polymer particles revealed an increase of up to 10.5% in mechanical strength compared with that of parts fabricated without plasma treatment of particles. This enhancement is likely due to the enhanced surface energy of the activated polymer particles, as well as the removal of moisture and/or organic contaminants on the polymer surface. To the best of our knowledge, this work is the first to report the use of plasma activation pre-treatments of polymer particles to achieve enhanced mechanical strength in injection-molded parts.

Table 2
C1s components on ABS polymer particles surface before and after plasma treatment %.

Samples	C—C/C—H	R—CN/C—O	—C═O	N—C═O
Before treatment	87.6	12.4		
Laboratory-scale reactor	82.7	13.2	2.2	1.9
Pilot-scale reactor	81.6	13.1	2.4	2.9

Table 3
C1s components on PP polymer particles surface before and after plasma treatment %.

Samples	C—C/C—H	C—O	C═O/O—C—O	O—CO—C
Before treatment	86.5	10.4		3.1
Laboratory-scale reactor	83.4	10.1	3.1	3.4
Pilot-scale reactor	77.8	12.5	5.8	3.9

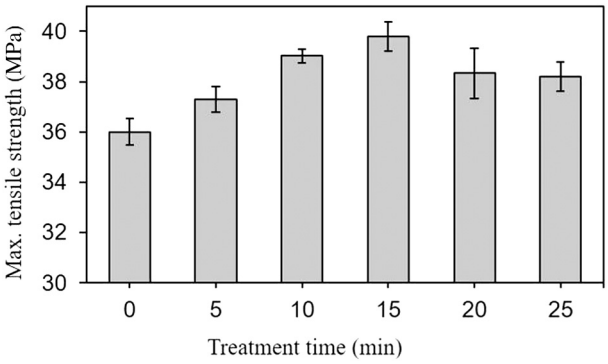

Fig. 13. Effect of plasma treatment time on the tensile strength of the injected molded parts.

Acknowledgments

The authors would like to acknowledge the support of the Enterprise Ireland Innovation Partnership program as well as the SFI funded I-Form Advanced Manufacturing Research Centre 16/RC/3872.

References

1. Oberbossel G, Güntner A, Kündig L, Roth C, von Rohr PR. Polymer powder treatment in atmospheric pressure plasma circulating fluidized bed reactor. Plasma Process Polym 2015;12:285-92. https://doi.org/10.1002/ppap.201400124.
2. Arefi-Khonsari F, Tatoulian M, Bretagnol F, Bouloussa O, Rondelez F. Processing of polymers by plasma technologies. Surf Coatings Technol 2005;200(1–4):14-20. https://doi.org/10.1016/j.surfcoat.2005.02.184. SPEC. ISS.
3. Abourayana H, Dowling D. Plasma processing for tailoring the surface properties of polymers. In: Aliofkhazraei M (ed); 2015. doi:https://doi.org/10.5772/60927.
4. Gilliam M, Farhat S, Zand A, Stubbs B, Magyar M, Garner G. Atmospheric plasma surface modification of PMMA and PP micro-particles. Plasma Process Polym 2014;11:1037-43. https://doi.org/10.1002/ppap.201300087.

5. Hunke H, Soin N, Shah T, Kramer E, Pascual A, Karuna MSL, Siores E. Low-pressure H_2, NH_3 microwave plasma treatment of polytetrafluoroethylene (PTFE) powders: chemical, thermal and wettability analysis. Materials (Basel) 2015;8:2258-75. https://doi.org/10.3390/ma8052258.
6. Morent R, De Geyter N, Leys C. Effects of operating parameters on plasma-induced PET surface treatment. Nucl Instruments Methods Phys Res Sect B Beam Interact with Mater Atoms 2008;266(12−13):3081-5. https://doi.org/10.1016/j.nimb.2008.03.166.
7. Put S, Bertels C, Vanhulsel A. Atmospheric pressure plasma treatment of polymeric powders. Surf Coatings Technol 2013;234:76-81. https://doi.org/10.1016/j.surfcoat.2013.02.006.
8. Arpagaus C, Sonnenfeld A, von Rohr PR. A downer reactor for short-time plasma surface modific ation of polymer powders. Chem Eng Technol 2005;28(1):87-94. https://doi.org/10.1002/ceat.200407045.
9. Vivien C, Wartelle C, Mutel B, Grimblot J. Surface property modification of a polyethylene powder by coupling fluidized bed and far cold remote nitrogen plasma technologies. Surf Interface Anal 2002;34:575-9. https://doi.org/10.1002/sia.1363.
10. Patra N, Hladik J, Pavlatová M, Militký J, Martinová L. Investigation of plasma-induced thermal, structural and wettability changes on low density polyethylene powder. Polym Degrad Stab 2013;98:1489-94. https://doi.org/10.1016/j.polymdegradstab.2013.04.014.
11. Fang S, Meng Y, Shen J, Cong J. Surface treatment of polypropylene powders using a plasma reactor with a stirrer. Plasma Sci Technol 2011;13:217-22. https://doi.org/10.1088/1009-0630/13/2/18.
12. Kim J-W, Kim Y, Choi H. Thermal characteristics of surface-crosslinked high density polyethylene beads as a thermal energy storage material. Korean J Chem Eng 2002;19:632-7. https://doi.org/10.1007/BF02699309.
13. Oberbossel G, Probst C, Giampietro VR, von Rohr PR. Plasma afterglow treatment of polymer powders: process parameters, wettability improvement, and aging effects. Plasma Process Polym 2017;14:1-10. https://doi.org/10.1002/ppap.201600144.
14. Abdul-Majeed WS, AL-Handhali IM, AL-Yaquobi SH, Al-Riyami KO. Application of novel polymeric surface remediation technique based on flying jet plasma torch. Ind Eng Chem Res 2017;56:11352-8. https://doi.org/10.1021/acs.iecr.7b02729.
15. Nakajima T, Tanaka K, Inomata T. Development of powder antifoamer by atmospheric pressure glow plasma. Thin Solid Films 2001;386:208-12. https://doi.org/10.1016/S0040-6090(00)01660-6.
16. Abourayana H, Barry N, Dobbyn P, Dowling D. Comparison between the performance of fluidized bed and barrel rectors for the plasma activation of polymer particles. J Miner Met Mater Eng 2015:57–64.
17. Abourayana H, Milosavljević V, Dobbyn P, Cullen P, Dowling D. Investigation of a scalable barrel atmospheric plasma reactor for the treatment of polymer particles. Surf Coatings Technol 2016;308:435-41. https://doi.org/10.1016/j.surfcoat.2016.06.094.
18. Abourayana H, Milosavljević V, Dobbyn P, Dowling D. Evaluation of the effect of plasma treatment frequency on the activation of polymer particles. Plasma Chem Plasma Process 2017;37:1223-35. https://doi.org/10.1007/s11090-017-9810-1.
19. Donegan M, Milosavljević V, Dowling D. Activation of PET using an RF atmospheric plasma system. Plasma Chem Plasma Process 2013;33:941-57. https://doi.org/10.1007/s11090-013-9474-4.
20. Thiyagarajan M, Sarani A, Nicula C. Optical emission spectroscopic diagnostics of a non-thermal atmospheric pressure helium-oxygen plasma jet for biomedical applications. J Appl Phys 2013;113:233302(1-8). https://doi.org/10.1063/1.4811339.
21. Xiong Q, Nikiforov AY, González MÁ, Leys C, Lu XP. Characterization of an atmospheric helium plasma jet by relative and absolute optical emission spectroscopy. Plasma Sources Sci Technol 2013;22, 015011. https://doi.org/10.1088/0963-0252/22/1/015011.
22. Milosavljevi V, Donegan M, Cullen P, Dowling D. *Diagnostics of an O_2–He RF atmospheric plasma discharge by spectral emission*,Vol. 014501 . 2014:1-8. https://doi.org/10.7566/JPSJ.83.014501.
23. Nersisyan G, Graham WG. Characterization of a dielectric barrier discharge operating in an open reactor with flowing helium. Plasma Sources Sci Technol 2004;13:582-7. https://doi.org/10.1088/0963-0252/13/4/005.
24. Sretenović G, Krstić I, Kovačević V, Obradović B, Kuraica M. Spectroscopic study of helium DBD plasma jet. IEEE Trans Plasma Sci 2012;40:2870-8. https://doi.org/10.1109/TPS.2012.2219077.
25. Nwankire CE, Law VJ, Nindrayog A, Twomey B, Niemi K, Milosavljević V, Graham WG, Dowling DP. Electrical, thermal and optical diagnostics of an atmospheric plasma jet system. Plasma Chem Plasma Process 2010;30:537-52. https://doi.org/10.1007/s11090-010-9236-5.
26. Mohan J, Ramamoorthy A, Ivanković A, Dowling D, Murphy N. Effect of an atmospheric pressure plasma treatment on the mode I fracture toughness of a co-cured composite joint. J Adhes 2014;90:733-54. https://doi.org/10.1080/00218464.2013.772053.
27. Soon J, Soung P, Dong L, Sang K. Surface modification of HDPE powders by oxygen plasma in a circulating fluidized bed reactor. Polym Bull 2001;47:199-205. https://doi.org/10.1007/s002890170012.
28. Pandiyaraj K, Selvarajan V, Deshmukh R, Changyou G. Adhesive properties of polypropylene (PP) and polyethylene terephthalate (PET) film surfaces treated by DC glow discharge plasma. Vacuum 2009;83:332-9. https://doi.org/10.1016/j.vacuum.2008.05.032.
29. Abenojar J, Torregrosa-Coque R, Martinez M, Martin-Martinez J. Surface modifications of polycarbonate (PC) and acrylonitrile butadiene styrene (ABS) copolymer by treatment with atmospheric plasma. Surf Coatings Technol 2009;203:2173-80. https://doi.org/10.1016/j.surfcoat.2009.01.037.
30. Kamińska A, Kaczmarek H, Kowalonek J. The influence of side groups and polarity of polymers on the kind and effectiveness of their surface modification by air plasma action. Eur Polym J 2002;38:1915-9. https://doi.org/10.1016/S0014-3057(02)00059-9.
31. Tahara M, Cuong NK, Nakashima Y. Improvement in adhesion of polyethylene by glow-discharge plasma. Surf Coatings Technol 2003;173–174:826-830. doi: 10.1016/S0257-8972.
32. Dowling D, O'Neill F, Langlais S, Law V. Influence of dc pulsed atmospheric pressure plasma jet processing conditions on polymer activation. Plasma Process Polym 2011;8:718-27. https://doi.org/10.1002/ppap.201000145.
33. Tsougeni K, Vourdas N, Tserepi A, Gogolides E, Cardinaud C. Mechanisms of oxygen plasma nanotexturing of organic polymer surfaces: from stable super hydrophilic to super hydrophobic surfaces. Langmuir 2009;25:11748-59. https://doi.org/10.1021/la901072z.
34. Wang C, He X. Polypropylene surface modification model in atmospheric pressure dielectric barrier discharge. Surf Coatings Technol 2006;201:3377-84. https://doi.org/10.1016/j.surfcoat.2006.07.205.
35. Gengenbach T, Griesser H. Post-deposition ageing reactions differ markedly between plasma polymers deposited from siloxane and silazane monomers. Polymer (Guildf) 1999;40:5079-94. https://doi.org/10.1016/S0032-3861(98)00727-7.
36. Dowling D, Tynan J, Ward P, Hynes A, Cullen J, Byrne G. Atmospheric pressure plasma treatment of amorphous polyethylene terephthalate for enhanced heatsealing properties. Int J Adhes Adhes 2012;35:1-8. https://doi.org/10.1016/j.ijadhadh.2012.01.025.
37. Rodriguez-Santiago V, Bujanda A, Stein B, Pappas D. Atmospheric plasma processing of polymers in helium-water vapor dielectric barrier discharges. Plasma Process Polym 2011;8:631-9. https://doi.org/10.1002/ppap.201000186.
38. Abourayana H, Dobbyn P, Dowling D. Enhancing the mechanical performance of additive manufactured polymer components using atmospheric plasma pretreatments. Plasma Process Polym 2017;15:1–8. doi:https://doi.org/10.1002/ppap.201700141.